ELSEVIER

Journal of Fluids and Structures 26 (2010) 841–847

JOURNAL OF FLUIDS AND STRUCTURES

www.elsevier.com/locate/jfs

Brief Communication

Static divergence of self-twisting composite rotors

Zhanke Liu*, Yin L. Young

Department of Naval Architecture and Marine Engineering, University of Michigan, Ann Arbor, MI 48109, USA

Received 5 December 2009; received in revised form 9 March 2010; accepted 10 May 2010

Abstract

Hydroelastic instabilities, such as static divergence and flutter, are major concerns for the safe operation of next-generation self-twisting composite marine rotors. In this paper, an efficient theoretical model was developed to obtain a first-order estimation of the static divergence speed of such rotors. The model was inspired by classical aeroelasticity theory and furnished with advanced numerical modeling. Its application to the marine environment was illustrated via a self-twisting composite propeller. The methodology is equally applicable to other structures, such as tidal and wind turbines.

Keywords: Hydroelasticity; Static divergence; Composite rotors

1. Introduction

Conventionally, marine propellers are made of metallic materials, such as nickel aluminum bronze (NAB). Composite marine propellers, which are made of carbon fiber reinforced plastics (CFRP), have several advantages over metallic propellers. First, they are lighter due to their higher specific strength and stiffness. Composite propellers also have better corrosion resistance due to the elimination of electrochemical cell set up. Most importantly, the deformation coupling behavior of anisotropic composites can be exploited to improve the propeller performance. The CFRP blades can be designed to rapidly and automatically adjust its pitch angle distribution as the flow changes by passive tailoring of the hydrodynamic load-induced deformations. Consequently, the propeller efficiency can be improved, cavitation can be delayed/reduced, when operating in off-design flow conditions or in a spatially varying wake. Moreover, the load variation can be reduced, which will also reduce the power demand and power variation, and hence improve the overall energy efficiency. Contrary to controllable pitch propellers, which require a mechanical driver and can only produce a constant change in pitch along the span, self-twisting composite marine propellers do not require any actuation device and the pitch angle change varies as a function of the blade radius and the hydrodynamic load.

The design, fabrication, and testing of a 24-in model-scale pitch-adapting composite marine propellers were presented in Chen et al. (2006). Results confirmed that a properly designed self-twisting composite marine propeller could be more efficient, and cavitation inception in wake inflow could be significantly delayed compared to its rigid counterpart under highly loaded off-design conditions. To exploit the benefits of self-twisting propellers, a systematic design methodology was proposed (Liu, 2008; Liu and Young, 2009). The methodology features a two-level design procedure. The first level

*Corresponding author.
E-mail address: zhankeliu2008@gmail.com (Z. Liu).

0889-9746/$ - see front matter © 2010 Elsevier Ltd. All rights reserved.
doi:10.1016/j.jfluidstructs.2010.05.002

is the material design which can be formulated as a multi-constraint optimization problem and tackled using an enhanced genetic algorithm equipped with numerical and analytical tools. The second level is the geometry design which can be formulated as an inverse problem and solved using an over-relaxed nonlinear iteration procedure. Sample designs and analysis presented in Liu and Young (2009), Motley et al. (2009), Young and Liu (2007) and Young et al. (2008) demonstrated the feasibility of desired performance enhancement over its rigid counterpart in uniform and spatially varying wake with and without cavitation.

Despite of their advantages during forward operations, the composite propellers' performance during crash-back operations still needs to be assessed. In general, there are four types of propeller operation modes. They are forward, backward, crash-ahead, and crash-back operations. The crash-back maneuver is to decelerate a ship by reversing the angular rotation of the propeller, which often results in the most extreme hydrodynamic loading (Jessup et al., 2006; Jiang et al., 1996; Vysohlid and Mahesh, 2006). The recent work by Chang et al. (2008) discussed the dynamic response and strength issues of metallic marine propellers subject to crash-back hydrodynamic loading. In addition to structural strength concerns, crash-back type loading may also lead to static divergence of self-twisting composite propellers as preliminarily discussed in Young et al. (2008). This is because the composite blades designed to de-pitch under forward operations will undergo an increase in pitch when the load reverses during crashback operations, which will tend to increase the hydrodynamic load and hence further increase the pitch. Consequently, structural instability and/or limit-state failure could be rapidly reached, which is the so-called static divergence. Thus it is crucial to investigate the potential hydroelastic instability behavior and failure mechanism of self-twisting composite propellers during crash-back operations.

The objective of the current work is to develop an efficient first-order model to predict the static divergence limit of self-twisting propellers subject to crash-back loading conditions.

2. Theoretical models

The analytical model is based on a classical hydrofoil model presented in Fung's classical textbook for torsional stability of a lifting surface (Fung, 1969). This model was proposed with the background of aeroelasticity. A typical 2-D (two-dimensional) hydrofoil is shown in Fig. 1. Notice that the 2-D hydrofoil has an equivalent elastic constraint to torsional deformation. It is used in the current paper to represent a typical cross-section of a propeller blade. For simplicity, the functional dependence on radius will be omitted in the formulations below. For more information about radial dependence of the pitch angle, the resultant inflow angle, and the effective angle of attack, the readers are referred to Liu and Young (2009). Based on the analysis by Fung (1969), the following relation holds to satisfy the torsional equilibrium:

$$qec^2a(\theta+\alpha_0)=K_\alpha\theta, \tag{1}$$

where $q=\rho U^2/2$ is the dynamic pressure, ρ is the fluid density, U is the resultant inflow speed, e is eccentricity of the aerodynamic center, c is the chord length, a is the slope of the hydrofoil lift-curve, α_0 is the initial angle of attack, θ is the angle of twist, and K_α is the torsional spring constant of the pivot. Notice that the angle α_0 is measured from the zero-lift line.

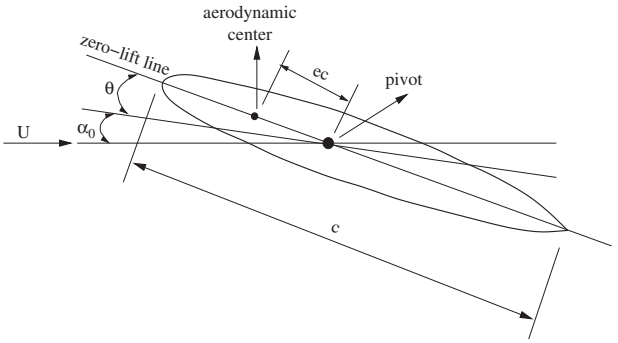

Fig. 1. A schematic two-dimensional hydrofoil.

Solving for θ using Eq. (1), we obtain

$$\theta = qec^2a\alpha_0/(K_\alpha - qec^2a). \tag{2}$$

For a given non-zero initial angle of attack α_0, the angle of twist θ becomes indefinitely large; the static divergence limit is reached when the dynamic pressure q is so large that the denominator in Eq. (2) approaches zero. Thus the condition of static divergence is given by

$$K_\alpha - qec^2a = 0, \tag{3}$$

which gives the divergence dynamic pressure

$$q_D = K_\alpha/(ec^2a). \tag{4}$$

Combination of Eqs. (2) and (4) gives

$$\frac{1}{\theta} = \frac{q_D}{\alpha_0}\left(\frac{1}{q} - \frac{1}{q_D}\right). \tag{5}$$

Using the relation $q_D = \rho U_D^2/2$, Eq. (5) can be expressed as follows:

$$\frac{1}{\theta} = \frac{U_D^2}{\alpha_0}\left(\frac{1}{U^2} - \frac{1}{U_D^2}\right). \tag{6}$$

Considering the centrifugal force (refer to Fung, 1969, Section 4.8), a slightly different version of Eq. (5) can be obtained:

$$\frac{1}{\theta} = \frac{q_D}{\alpha_0 - \alpha_c}\left(\frac{1}{q} - \frac{1}{q_D}\right), \tag{7}$$

where θ is the angle of twist due to elasticity, α_0 is the initial angle of attack, and α_c is the angle of attack for zero twist, which can be calculated from the equilibrium of aerodynamic/hydrodynamic force and the centrifugal force. Notice that both α_0 and α_c are measured from the zero-lift line (Fung, 1969).

Using the relation $q_D = \rho U_D^2/2$, Eq. (7) can be expressed as follows:

$$\frac{1}{\theta} = \frac{U_D^2}{\alpha_0 - \alpha_c}\left(\frac{1}{U^2} - \frac{1}{U_D^2}\right). \tag{8}$$

It can be seen from Eqs. (6) or (8) that there exists a linear relation between $1/\theta$ and $1/U^2$. If $1/\theta$ is plotted against $1/U^2$, a straight line is expected. The intercept of the straight line with the $1/U^2$ axis should be $1/U_D^2$. Although marine propeller blades involve complex 3-D geometry, the bending and twisting deformation at each radial section are smooth functions of the blade radii, and hence can be related to the 2-D behavior at the blade tip. If θ and U are taken as the angle of twist (represented by the change in pitch angle) and the resultant inflow speed, both at the blade tip, then the model given by Eq. (8) can be applied to a realistic propeller as long as the two quantities can be conveniently obtained. Notice that Eqs. (6) and (8) have a similar structure and they yield exactly the same results in the determination of the static divergence speed. They only differ in the slopes of the linear curve, with Eq. (8) accounting for the centrifugal effects. It should be noted that the numerical solver used in the current paper does account for the effect of centrifugal force, which is consistent with Eq. (8).

Once the divergence resultant inflow speed U_D is obtained, the divergence ship speed U_s can be calculated as

$$U_s = \sqrt{U_D^2 - (\pi nD)^2}, \tag{9}$$

where n and D are the propeller rotational speed and propeller diameter, respectively.

Eq. (5) was recommended in Fung (1969) as a convenient formula to obtain from experiments the divergence speed of lifting surfaces with torsional stiffness. In the current work, a numerical approach was adopted instead. The numerical tool is a three-dimensional fluid–structure interaction solver for marine propellers (Young, 2007, 2008). Basically, the blade, hub, and wake surfaces are discretized using hyperboloidal panels and the fluid velocity potential, pressure distributions, and cavitation patterns are solved using a low-order potential-based 3-D boundary element method (BEM) in the time-domain. The solid blade structure is discretized using 3-D quadratic continuum elements, and is

solved in the time-domain using a finite element method (FEM). The hydrodynamic pressure obtained from the BEM is applied on the solid FEM mesh as surface tractions, and the structural deformation is solved using the FEM. The influence of fluid–structure interaction is considered by superimposing the hydrodynamic added mass and damping matrices to the structural added mass and damping matrices, and by iterating between the BEM and FEM solvers to account for the effect of nonlinear blade deformation. Additional details about the coupled BEM–FEM model can be found in Young (2007, 2008).

3. Results and discussion

To demonstrate the proposed theoretical model, and to investigate the static divergence behavior of self-twisting composite marine propellers, a numerical example is presented below.

The initial geometry was taken to be that of propeller 5474M, which has the same no-load geometry (the manufactured geometry without hydrodynamic load-deformations) as propeller 5474 (Liu, 2008; Young et al., 2008), one of the pair of composite marine propellers designed and tested by the Naval Surface Warfare Center, Carderock Division (Chen et al., 2006). The propeller has a diameter $D = 2\,\text{ft} = 0.6096\,\text{m}$. It was designed for the advance coefficient $J = V/(nD) = 0.66$, rotational speed $n = 780\,\text{rpm}$, and propeller advancing speed $V = 5.23\,\text{m/s}$. Due to proprietary issues, instead of using the actual material, the blades were assumed to be made of carbon/epoxy T300/5208, which has a density of $\rho_s = 1500\,\text{kg/m}^3$, longitudinal Young's modulus of $E_1 = 171.42\,\text{GPa}$, transverse Young's modulus of $E_2 = 9.08\,\text{GPa}$, shear modulus of $G_{12} = 5.29\,\text{GPa}$, and Poisson's ratio of $\nu_{12} = 0.32$. The propeller with the modified material is called 5474M to distinguish it from the original propeller 5474. The discretized geometry of propeller 5474M is shown in Fig. 2. For illustration purposes, the fiber orientation is assumed to be $\alpha = +30^\circ$ in the counter-clockwise direction from the local span-wise coordinates. Propeller 5474M was designed to automatically de-pitch under hydrodynamic load during normal forward operations. The $+30^\circ$ fiber orientation was designed to de-pitch in an almost linear manner under increasing load in forward operating conditions. Thus, a -30° construction would result in an increase in pitch under the same increase in load in forward operating conditions. The increased pitch will lead to higher hydrodynamic loading and further increase the pitch angle, quickly approaching the state of static divergence. This is very similar to the problem that occurs for the $+30^\circ$ propeller during crashback, except for the switch in leading edge and trailing edge, and the large-scale vortices generated by competing flows. To simulate the increasing pitch behavior under crashback loading conditions, the fiber orientation angle is reversed, i.e. the fibers are assumed to be aligned at $\alpha = -30^\circ$ in the clockwise direction from the local span-wise coordinates. Parametric studies were also performed for $\alpha = -35^\circ$, and for $\alpha = -40^\circ$. Steady flow conditions were assumed for all the simulations.

A series of pairs of numerical results for $(1/\theta, 1/U^2)$ can be obtained by varying the propeller rotational speed n while keeping the same advance coefficient J. As shown in Fig. 3, $1/\theta$ is plotted as a function of $1/U^2$. The numerical results

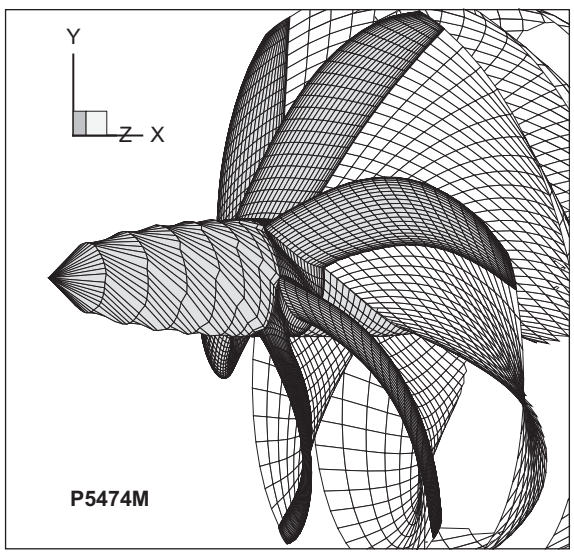

Fig. 2. The discretized geometry of propeller 5474M.

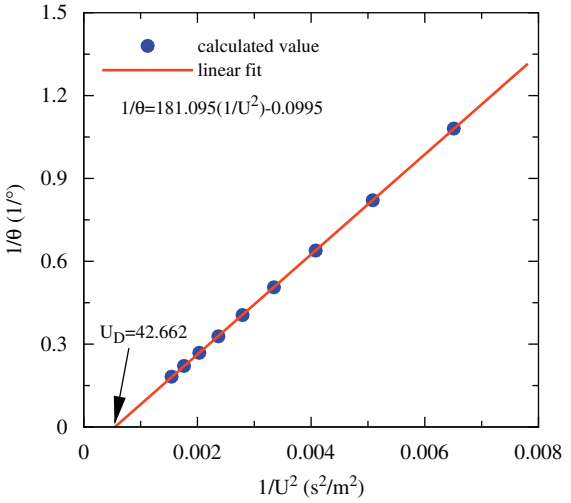

Fig. 3. Determination of the resultant divergence inflow speed U.

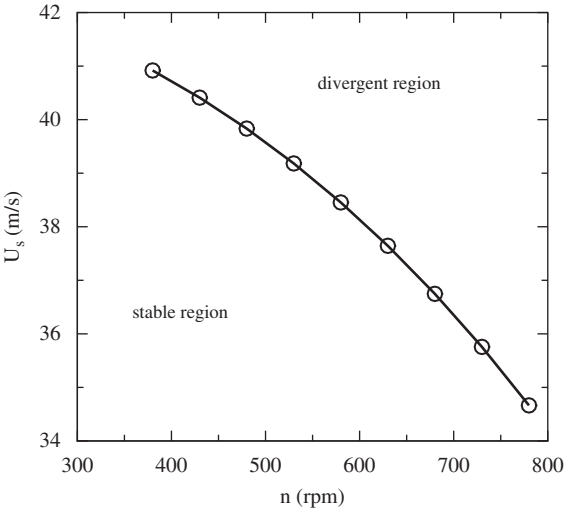

Fig. 4. Estimated divergence ship speed U_s.

are denoted by dots. Notice that nine pairs of data are presented. The rotational speed n varies from 380 to 780 rpm by increments of 50 rpm. A straight line was obtained based on $R^2 = 0.999987$, indicating a strong linear fit with negligible scatter. By using the intercept of the fitted line with the $1/U^2$ axis, the resultant divergence inflow speed U_D can be obtained. The divergence ship speed U_s can be calculated using the relation given in Eq. (9). As shown in Fig. 4, the divergence ship speed U_s is plotted as a function of the propeller rotational speed n. The divergence ship speed monotonically decreases with the increasing of the propeller rotational speed as expected from Eq. (9).

Parametric studies were performed for varying fiber orientations, $\alpha = -30^\circ$, -35°, and -40°. As shown in Fig. 5, the divergence ship speed U_s varies with the fiber orientations α. It can be seen that $\alpha = -30^\circ$ leads to the lowest static divergence speed, which shows that $\alpha = -30^\circ$ corresponds to the lowest torsional stiffness, since U_D (and thus U_s) is proportional to the square root of the equivalent torsional stiffness (K_α) of the propeller, as indicated by Eq. (4). Also plotted in Fig. 5 are the changes in tip pitch angle $\Delta\phi$ for the self-twisting propeller under the fixed advance coefficient $J = 0.66$ for various rotational speed n. Notice that they follow the opposite trend compared to the divergence ship speed U_s. Basically, they increase with the increasing value of the rotational speed. This is because the dimensional hydrodynamic load increases with the square of the rotational speed n for a fixed advance coefficient J. At the same

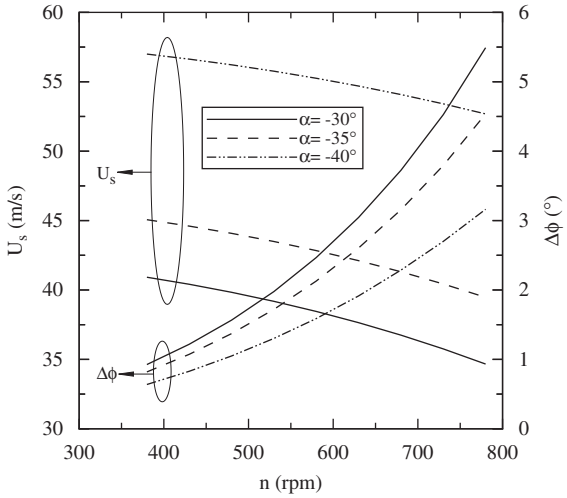

Fig. 5. Correlation between the divergence ship speed (U_s) and the change in the tip pitch angle ($\Delta\phi$).

time, $\alpha = -30^\circ$ leads to the maximum change in the tip pitch angle, which is consistent with what observed for the divergence ship speed as shown in the same figure.

4. Conclusion

An efficient approach was proposed in the current work for the calculation of the static divergence speed of self-twisting composite marine rotors. It was inspired by an analytical model presented in the literature, which is used in this work along with a numerical propeller fluid–structure interaction analysis model developed by the authors (Young, 2007, 2008). The simplified model by Fung (1969) considers a generalized 2-D hydrofoil with elastic torsional constraint and centrifugal effects. The 3-D fluid–structure interaction solver of Young (2007, 2008) is a sophisticated coupled iterative BEM–FEM model that accounts for steady and unsteady flow, centrifugal and Coriolis forces, blade wake interactions, complex blade geometries, geometric structural nonlinearities and nonlinear changes in pitch, rake and skew due to fluid–structure interactions. The combined analytical–numerical model provides an efficient first-order estimation of the upper speed limit for the safe operation of self-twisting composite marine propellers during crash-back operation. A strong correlation was identified between the divergence ship speed and the change in the tip pitch angle of the blades. Both quantities are closely related to the equivalent torsional stiffness of the self-twisting propeller. Thus, the torsional stiffness should be included as a constraint in the optimization of composite marine propellers for safety considerations. The current approach serves as an important tool for the preliminary design and analysis of next-generation self-twisting composite marine propellers. However, it should be remembered that the static divergence model was based on a simplified hydrofoil configuration and that the current potential-based fluid solver does not account for the effects of large-scale asymmetric vorticities that develop near the blade tips as observed in experimental studies of crashback operations. High-fidelity flow simulation coupled with more advanced static divergence modeling warrants further investigation. Nevertheless, it is important to emphasize that a fully coupled 3-D model that considers the complex interactions between deformation behavior of a self-twisting composite propeller and turbulent, vortical flow during crashback will be very computationally expensive. Hence, it is much more practical to use the proposed method in the design and optimization process, and use a high-fidelity coupled FSI solver in the post-design process to ensure structural integrity.

Acknowledgments

The authors are grateful to the Office of Naval Research (*ONR*) and Dr Ki-Han Kim (Program Manager) for their financial support through Grant numbers N00014-05-1-0694, N00014-07-1-0491, and N00014-08-1-0475.

References

Chang, P.A., Ebert, M., Young, Y.L., Liu, Z., Mahesh, K., Jang, H., Shearer, E.M., 2008. Propeller forces and structural response due to crashback. In: 27th Symposium on Naval Hydrodynamics, Seoul, Korea.

Chen, B., Neeley, S., Michael, T., Gowing, S., Szwerc, R., Buchler, D., Schult, R., 2006. Design, fabrication and testing of pitch-adapting (flexible) composite propellers. In: 2006 SNAME Propeller/Shafting Symposium, VA, USA.

Fung, Y., 1969. An Introduction to the Theory of Aeroelasticity. Dover, New York.

Jessup, S., Fry, D., Donnelly, M.J., 2006. Unsteady propeller performance in crashback conditions with and without a duct. In: 26th Symposium on Naval Hydrodynamics, Rome, Italy.

Jiang, C.W., Dong, W., Liu, H.L., Chang, M.S., 1996. 24-in water tunnel flow field measurements during propeller crashback. In: 21st Symposium on Naval Hydrodynamics, Trondheim, Norway.

Liu, Z., 2008. Transient analysis and design of composite structures in multiphase flows. Ph.D. Thesis, Princeton University.

Liu, Z., Young, Y.L., 2009. Utilization of bend–twist coupling for performance enhancement of composite marine propellers. Journal of Fluids and Structures 25.

Motley, M.R., Liu, Z., Young, Y.L., 2009. Utilizing fluid–structure interactions to improve energy efficiency of composite marine propellers in spatially varying wake. Composite Structures 90.

Vysohlid, M., Mahesh, K., 2006. Large eddy simulation of crashback in marine propellers. In: 26th Symposium on Naval Hydrodynamics, Rome, Italy.

Young, Y.L., 2007. Time-dependent hydroelastic analysis of cavitating propeller. Journal of Fluids and Structures 23.

Young, Y.L., 2008. Fluid–structure interaction analysis of flexible composite marine propellers. Journal of Fluids and Structures 24.

Young, Y.L., Liu, Z., 2007. Hydroelastic tailoring of composite naval propulsors. In: 26th International Conference on Offshore Mechanics and Arctic Engineering, San Diego, CA, USA.

Young, Y.L., Liu, Z., Motley, M.R., 2008. Influence of material anisotropy on the hydroelastic behaviors of composite marine propellers. In: 27th Symposium on Naval Hydrodynamics, Seoul, Korea.